HCK is a survival determinant transactivated by mutated MYD88, and a direct target of ibrutinib

Yang, Guang; Buhrlage, Sara; Tan, Li; Liu, Xia; Chen, Jie; Xu, Lian

Published in:
Blood

DOI:
10.1182/blood-2016-01-695098

Publication date:
2016

Document Version
Peer reviewed version

HCK is a survival determinant transactivated by mutated MYD88, and a direct target of ibrutinib.

Guang Yang,[1] Sara Buhrlage,[2] Tan Li,[2] Xia Liu,[1] Jie Chen,[1] Lian Xu,[1] Nicholas Tsakmaklis,[1] Jiaji G. Chen,[1] Christopher J. Patterson,[1] Jennifer R. Brown,[3] Jorge J. Castillo,[1] Wei Zhang,[4] Xiaofeng Zhang,[4] Shuai Liu,[4] Philip Cohen,[5] Zachary R. Hunter,[1] Nathanael Gray,[2] and Steven P. Treon.[1]

[1]Bing Center for Waldenstrom's Macroglobulinemia, Dana Farber Cancer Institute and Harvard Medical School; [2]Department of Biological Chemistry and Molecular Pharmacology, Harvard Medical School, Boston MA USA; [3]Department of Medical Oncology, Dana Farber Cancer Institute and Harvard Medical School; [4]University of Massachusetts, Boston MA USA; and [5]University of Dundee, Dundee Scotland UK.

Corresponding author:
Steven P. Treon, M.D., Ph.D.
Bing Center for Waldenström's Macroglobulinemia
Dana Farber Cancer Institute
M548, 450 Brookline Avenue, Boston, MA 02115 USA
Tel: (617) 632-2681 Fax: (617) 632-4862
Email: steven_treon@dfci.harvard.edu

Short Title: HCK is a target of Ibrutinib.
Abstract Word Count: 228
Text Word Count: 4287
Tables: 0 **Figures**: 7
Keywords: Waldenstrom macroglobulinemia, ABC DLBCL, HCK, MYD88 L265P, Ibrutinib.

Keypoints

- HCK transcription and activation is triggered by mutated MYD88, and is an important determinant of pro-survival signaling.
- HCK is also a target of ibrutinib, and inhibition of its kinase activity triggers apoptosis in mutated MYD88 cells.

Abstract

Activating mutations in MYD88 are present in approximately 95% of patients with Waldenstrom Macroglobulinemia (WM), as well as other B-cell malignancies including ABC DLBCL. In WM, mutated MYD88 triggers activation of BTK. Ibrutinib, a pleiotropic kinase inhibitor that targets BTK, is highly active in patients with mutated MYD88. We observed that mutated MYD88 WM and ABC DLBCL cell lines, as well as primary WM cells show enhanced HCK transcription and activation, and that HCK is activated by IL6. Over-expression of mutated MYD88 triggers HCK and IL6 transcription, while knockdown of HCK reduced survival and attenuated BTK, PI3K/AKT, and MAPK/ERK signaling in mutated MYD88 WM and/or ABC DLBCL cells. Ibrutinib and the more potent HCK inhibitor A419259 blocked HCK activation and induced apoptosis in mutated MYD88 WM and ABC DLBCL cells. Docking and pull-down studies confirmed that HCK was a target of ibrutinib. Ibrutinib and A419259 also blocked ATP binding to HCK, while transduction of mutated MYD88 expressing WM cells with a mutated HCK gatekeeper greatly increased the EC_{50} for ibrutinib and A419259. The findings support that HCK expression and activation is triggered by mutated MYD88, supports the growth and survival of mutated MYD88 WM and ABC DLBCL cells, and is a direct target of ibrutinib. HCK represents a novel target for therapeutic development in MYD88 mutated WM and ABC DLBCL, and possibly other diseases driven by mutated MYD88.

Introduction

Next generation sequencing has revealed activating MYD88 mutations in several B-cell malignancies. Particularly striking has been the expression of MYD88 mutations in Waldenstrom Macroglobulinemia (WM), wherein 95-97% of patients express $MYD88^{L265P}$, and more rarely non-L265P MYD88 mutations.[1-4] Up to 30% of patients with activated B-cell (ABC) subtype of diffuse large B-cell lymphoma (ABC DLBCL) also express activating MYD88 mutations, including $MYD88^{L265P}$.[5,6] Mutations in MYD88 promote Myddosome self-assembly and can trigger NF-kB signaling in the absence of Toll (TLR) or IL1 (IL1R) receptor signaling through IL1 Receptor Associated Kinases (IRAK4/IRAK1) or Bruton's Tyrosine Kinase (BTK).[5,7]

Ibrutinib is a pleiotropic kinase inhibitor that is known to target BTK, and is highly active in previously treated WM patients producing an overall response rate of 91%.[8] In WM patients, both major and overall responses to ibrutinib are higher in patients with MYD88 mutations.[9] CXCR4 WHIM mutations that are present in up to 40% of WM patients can also impact ibrutinib response.[4] Ibrutinib also shows activity in previously treated patients with ABC-DLBCL, particularly among patients with BCR pathway and MYD88 mutations.[10] Ibrutinib is also active in other B-cell malignancies including CLL and MCL. Suppression of tonic B-cell receptor (BCR) activity mediated by BTK has been implicated as the mechanism underlying ibrutinib activity in non-WM B-cell diseases.

In addition to BTK, ibrutinib can suppress the activity of several other kinases including members of the SRC family.[11] Hematopoietic cell kinase (HCK) is a member of the SRC family of protein tyrosine kinases, and one of the most aberrantly up-regulated genes in WM cells.[12] In myeloma cells, HCK is activated by interleukin 6 (IL6) through the IL6 co-receptor IL6ST (GP130).[13,14] IL6 is also a potent growth and survival factor in WM, though the functional significance of HCK in WM pathogenesis remains unclear.[15] We therefore investigated the role of

HCK in WM, and impact of MYD88 mutations and ibrutinib on the transcriptional regulation and activation of this SRC family member.

Materials and Methods

Primary cells and cell lines

Primary WM cells ($CD19^{+}$) were isolated from bone marrow (BM) aspirates, and peripheral blood mononuclear cells (PBMC) were collected from healthy donors (HD) after informed written consent. Primary WM lymphoplasmacytic cells (LPC) and cell lines were genotyped for MYD88 and CXCR4 mutations as previously described.[2,4] $MYD88^{L265P}$ BCWM.1 and MWCL-1 WM cells; TMD-8, HBL-1, and OCI-Ly3 and $MYD88^{S122R}$ SU-DHL2 ABC DLBCL cells; and MYD88 wild-type ($MYD88^{WT}$) OCI-Ly7 and OCI-Ly19 germinal center B-cell (GCB) DLBCL cells; Ramos Burkitt's cells; and RPMI-8226 and MM.1S myeloma cells were used.

Lentiviral transduction experiments

$MYD88^{WT}$ or $MYD88^{L265P}$ proteins were over-expressed in BCWM.1 and MWCL-1 cells following lentiviral transduction as previously described.[7] The over-expression of proteins coding for wild-type HCK (HCK^{WT}) or HCK harboring a mutated gatekeeper residue (HCK^{T333M}) at amino acid position 333 (338 based on c-SRC numbering)[16] was accomplished by lentiviral transduction of HCK^{WT} or HCK^{T333M} (r. 1235C>T in NM_002110.3) sequences in a pLVX-EF1α-IRES-Puro vector (Clontech Laboratories, Mountain View CA). Knockdown of HCK or IL6ST (GP130) was performed using an inducible the lentiviral shRNA expression vector pLKO-Tet-On containing a tetracycline regulated expression cassette (Addgene, Cambridge MA). Following lentiviral transduction of BCWM.1 and MWCL-1 cells, stable cell lines were selected with 0.5~1.0 ug/ml puromycin in tetracycline-free medium. For the induced knockdown of HCK or IL6ST, tetracycline (0.8 ug/ml) was added to culture media. For HCK knockdown, lentiviral vectors were

designed to target 5'-GCTGTGATTTGGAAGGGAA-3' (HCK shRNA1) and 5'-GGATAGCGAGACCACTAAA-3' (HCK shRNA2). IL6ST knockdown targeted 5'-GGAGCAATATACTATCATA-3' (IL6ST shRNA1) and 5'-GGAACTGTCTAGTATCTTA-3' (IL6ST shRNA2). A scrambled shRNA vector was used for control purposes.

Cell viability assessments

Apoptosis analysis was performed using Annexin V/Propidium iodide staining with the Apoptosis Detection Kit I (BD Pharmingen, San Jose CA). Cells (1×10^6/well) were treated in 24 well plates for 18 hours with inhibitors or corresponding controls. A minimum of 10,000 events were acquired using a BD™ FACSCanto II flow cytometer, and analyzed with BD FACS DIVA Software. For WM patient cells, BMMC (2×10^6/well) were treated with inhibitors, and CD19-APC-cy7 antibody (BD Pharmingen) was used with Annexin V antibody to analyze WM cell apoptosis. AlamarBlue® cell viability assay (Life Technologies, Carlsbad CA) was used to assess cell death following inducible HCK knockdown. For these experiments, transduced cells (1×10^5/ml) were cultured with tetracycline, and aliquoted every other day on days 1-11. AlamarBlue® solution (1/10 total volume) was added to cells and incubated for 2 hours. Aliquoted plates were read in a SpectraMax M3 plate reader (Molecular Devices, Sunnyvale, CA). Relative cell survival was calculated as percentage of fluorescence relative to scrambled control. The CellTiter-Glo® Luminescent cell viability assay (Promega, Madison WI) was used to assess the dose-response of inhibitors. Cells were seeded into 384 well plates with the EL406 Combination Washer Dispenser (BioTek Instruments, Inc.) and inhibitors injected into the cells culture media with the JANUS Automated Workstation (PerkinElmer Inc., Waltham MA). Cells were treated with serial diluted inhibitors (20~0.0006μM) for 72 hours at 37^o C. Luminescent measurement was performed using the 2104 Envision® Multilabel Reader (PerkinElmer Inc.).

RT-PCR and quantitative-PCR

Total RNA were isolated using AllPrep DNA/RNA Mini Kit (QIAGEN), and cDNA synthesized by SuperScript® III First-Strand Synthesis SuperMix (Life Technologies). Quantitative detection of mRNA levels for HCK, IL6 and IL6R was performed using TaqMan® Gene Expression Assays with TaqMan® Gene Expression Master Mix per manufacturer's instructions using the ABI Prism 7500 Sequence Detection System (Applied Biosystems). HCK transcription was also assessed two hours following incubation with either IL6 (1-10 ng/mL) or IL6 blocking antibody (1-10 ug/mL) (both from R&D Systems, Minneapolis MN) in BCWM.1 and MWCL-1 cells by quantitative RT-PCR.

PhosFlow analysis

PhosFlow analysis was performed to delineate HCK phosphorylation. Cells were fixed with BD PhosFlow Fix Buffer I at 37ºC for 10 min. Cells were then centrifuged (300×g for 5 min) and washed twice with PhosFlow Perm/Wash Buffer I (BD Pharmingen). Cells were then stained with HCK ($pTyr^{411}$) antibody (Abcam, Cambridge MA) alone (for cell lines) or with anti-CD20-APC-Cy7 (BD Pharmingen) for primary WM cells. Following staining, cells were incubated in the dark for 30 min at room temperature, then washed thrice with BD PhosFlow Perm/Wash Buffer I, followed by anti-Rabbit IgG DyLight®-649 secondary antibody (Abcam), and incubated for an additional 20 min. Cells were then washed twice with BD PhosFlow Perm/Wash Buffer I and flow analysis performed using a BD™ FACSCanto II Flow Cytometer.

Immunoblotting

Immunoblotting was performed following gene over-expression, knockdown or kinase pulldown with biotinylated probes using antibodies for HCK, AKT-pT308, AKT, ERK1/2-pT202/pY204, ERK1/2, PLCγ1-pY783, PLCγ2-pY1217, PLCγ2,

BTK-pY223, BTK, IRAK4-pT345/S346, IRAK4, SRC, LYN (Cell Signaling Technologies, Danvers MA), PI3K-p85β-pY464 (LifeSpan Biosciences, Seattle WA), PI3K-p85β, PLCγ1, IL6ST (Santa Cruz Biotechnology, Dallas TX) in primary WM cells, and cell lines. Staining with GAPDH antibodies was used for determination of protein loading (Santa Cruz Biotechnology).

Ibrutinib probe assay and kinase active-site inhibition assay

For Ibrutinib probe assay, BCWM.1, MWCL-1 or TMD-8 cells (2×10^7) were treated with ibrutinib-biotin or CC-292-biotin (2 uM) for 1 hour. Cells then washed with PBS twice, and lysed with co-IP buffer (Invitrogen, Grand Island NY). Two mg of protein from lysed cells was then incubated with 50 ul of Pierce Streptavidin Magnetic Beads (Thermo Fisher Scientific, Cambridge MA) at 4ºC for 1 hour, then washed with TBST (0.1% Tween-20) thrice, and proteins eluted with SDS-PAGE sample buffer. For Kinase active-site inhibition assay, BCWM.1 cells (2×10^7) were pre-treated with DMSO, ibrutinib, CC-292 or A419259 (MedChem Express, Monmouth Junction NJ) at various concentrations for 1 hour. Cells then were lysed and kinases were pulled down with ATP-biotin using Pierce™ Kinase Enrichment Kit (Thermo Fisher Scientific) per manufacturer's instructions. Kinases were eluted with SDS-PAGE sample buffer and detected by western blot.

Docking study

The docking studies were performed using AutoDockTools 1.56[17], AutoDock VINA[18] and Open Babel[19] software. The lowest calculated Gibbs energy (ΔG) of the predicted binding modes indicates stronger binding affinity, and binding modes with ΔG lower than -10 kcal are highly probable to be true.

Statistical analysis

The statistical significance of differences was analyzed using One-way ANOVA with Tukey's multiple comparisons test by Prism software. Differences were considered significant when $p<0.05$.

Results

HCK transcription is driven by mutated MYD88.

To clarify if HCK expression was aberrant in MYD88 mutated cells, we first assessed HCK transcription in MYD88 mutated WM and DLBCL cell lines by TaqMan® Gene Expression Assay. The results showed that HCK was markedly transcribed in $MYD88^{L265P}$ expressing WM (BCWM.1, MWCL-1) and DLBCL (TMD-8, HBL-1, OCI-Ly3) cells, but absent or at very low levels in $MYD88^{WT}$ (OCI-Ly7, OCI-Ly19, Ramos, MM1.S and RPMI-8226) cells by quantitative RT-PCR (Figure 1A). Expression of the HCK transcript was also enhanced in SU-DHL2 cells that carry the $MYD88^{S122R}$ activating mutation. Western blot analysis confirmed enhanced HCK protein expression in MYD88 mutated cell lines (Figure 1A). We next investigated the mRNA levels of HCK in $MYD88^{L265P}$ genotyped CD19-sorted primary WM cells using a TaqMan® Gene Expression Assay. We compared HCK expression levels to both sorted healthy donor derived non-memory ($CD19^{+}CD27^{-}$) and memory ($CD19^{+}CD27^{+}$) B-cells, given that the later represent the B-cell population from where most cases of WM are likely derived.[20,21] The HCK transcript was elevated in $MYD88^{L265P}$ WM cells versus either healthy donor non-memory or memory B-cells (Figure 1B). CXCR4 mutation status did not impact HCK transcription in primary WM cells ($p=0.90$ for CXCR4 wild-type versus WHIM mutated patients). To clarify if mutated MYD88 was responsible for enhanced HCK expression, we over-expressed $MYD88^{L265P}$ or $MYD88^{WT}$ protein in $MYD88^{L265P}$ BCWM.1 and MWCL-1 cells, and $MYD88^{WT}$ OCI-Ly9 and Ramos cells, and assessed for differences in HCK transcription. By Western blot analysis, similar levels of exogenous MYD88 protein were detectable in $MYD88^{L265P}$ or $MYD88^{WT}$ transduced cells (Figure 1C). The results of these

studies showed significantly higher levels of HCK transcript in all four cell lines following over-expression of MYD88^{L265P} versus MYD88^{WT} protein (Figure 1C).

IL6 but not IL6R transcription is induced by mutated MYD88.

Since previous work showed that HCK was activated by IL6 via IL6R/IL6ST, we investigated the regulatory role of mutated MYD88 on IL6 and IL6R expression.[13,14] By quantitative RT-PCR, IL6 transcription was markedly higher in MYD88^{L265P} expressing WM (BCWM.1, MWCL-1) and DLBCL (TMD-8, HBL-1, OCI-Ly3), as well as MYD88^{S122R} expressing SU-DHL2 cells versus MYD88^{WT} (OCI-Ly7, OCI-Ly19, Ramos, MM1.S and RPMI-8226) cells (Figure 2A). Similarly, IL6R transcription was increased in MYD88 mutated cell lines. Among MYD88^{WT} malignant B-cells, IL6R transcription was low or absent, though was highly expressed in MYD88^{WT} malignant plasma cells (Figure 2B). By TaqMan® Gene Expression Assay, higher IL6 (Figure 2C) and IL6R (Figure 2D) transcription were found in MYD88^{L265P} WM samples versus healthy donor non-memory ($CD19^{+}CD27^{-}$) and memory ($CD19^{+}CD27^{+}$) B-cells. Given these findings, we next sought to clarify if MYD88^{L265P} was a driver for IL6 and IL6R transcription. Over-expression of the MYD88^{L265P} protein induced marked IL6 (Figure 2E), but not IL6R (Figure 2F) transcription in MYD88^{L265P} (BCWM.1, MWCL-1) and MYD88^{WT} (OCI-Ly9 and Ramos) cells. Conversely, over-expression of MYD88^{WT} protein had little or no impact on IL6 or IL6R transcription.

HCK is hyperactive in MYD88 mutated cells, and its activation but not transcription is triggered by IL6.

Given the above findings, we next investigated the activation state of HCK in MYD88 mutated WM and DLBCL cell lines, and primary WM cells. By PhosFlow analysis, HCK showed consistently high phosphorylation levels at the Tyr^{411} activation site in mutated MYD88 versus wild-type MYD88 cells (Figure 3A). Significantly higher levels of HCK Tyr^{411} phosphorylation were also observed in

primary WM patient samples versus healthy donor non-memory and memory B-cells (Figure 3B). CXCR4 mutation status was available for 18 of 20 primary WM patient samples, and did not impact HCK Tyr^{411} phosphorylation (p=0.65 for CXCR4 wild-type versus WHIM mutated patients). Treatment of mutated MYD88 WM and DLBCL cell lines and primary WM lymphoplasmacytic cells (LPCs) with IL6 augmented HCK activation, with a peak induction of Tyr^{411} phosphorylation at 5 minutes following IL6 administration in mutated MYD88 cells (Figure 3C). In contrast, little or no effect on HCK Tyr^{411} phosphorylation was observed following IL6 stimulation in $MYD88^{WT}$ cells. Knockdown of IL6ST attenuated HCK activation in the presence or absence of IL6, whereas transduction with a control vector had little or no impact on HCK activation in MYD88 mutated BCWM.1 cells (Figure 3D). Lastly, HCK transcription was not significantly altered following incubation with either IL6 (1-10 ng/mL) or an IL6 blocking antibody (1-10 ug/mL) for two hours in BCWM.1 and MWCL-1 cells using RT-PCR (data not shown).

HCK is a determinant of survival in MYD88 mutated cells

We next evaluated the impact of HCK expression on survival in MYD88 mutated BCWM.1 and MWCL-1 WM and TMD-8 and HBL-1 ABC DLBCL cells. Successful knockdown of HCK was accomplished by lentiviral transduction using inducible shRNA vectors (Figure 4A). The results of these studies showed that knockdown of HCK in all 4 MYD88 mutated cell lines by either of two shRNA vectors resulted in sustained reduction in tumor cell viability over the 9 day evaluation period in contrast to cells transduced with a control vector (Figure 4B).

HCK triggers pro-survival signaling in MYD88 mutated WM cells.

In view of the above findings, we next interrogated HCK dependent survival signaling in MYD88 mutated WM cells. We focused our efforts on PI3K/AKT, MAPK and BTK signaling pathways given their established importance in WM survival, as well as previous work implicating HCK as an upstream regulator for their signaling.[22-25] Transduction of HCK in IL6 producing BCWM.1 and MWCL-1

cells led to higher HCK protein levels by Western blot analysis and detection of activated HCK (Tyr^{411}) by PhosFlow analysis (Figure 5A, 5B). Transduction of HCK in BCWM.1 and MWCL-1 cells also triggered PI3K/AKT (pPIK3R2, pAKT), MAPK (pPLCγ1, pERK1/2), and BTK (pBTK, pPLCγ2) signaling (Figure 5B), whereas knockdown of HCK in BCWM.1 and MWCL-1 cells showed a reciprocal pattern, with diminished PI3K/AKT, MAPK and BTK signaling (Figure 5C). IRAK4 activation was not impacted by either HCK over-expression or knockdown. Total protein levels for these signaling molecules, and GAPDH remained unchanged in these experiments.

Ibrutinib binds to the ATP-binding pocket of HCK and blocks ATP binding.

Kinase selectivity profiling has established that in addition to being a covalent inhibitor of BTK, ibrutinib is also a potent non-covalent inhibitor of several SRC family members including HCK, YES and LCK.[11] We focused our attention on investigating the potential functional significance of HCK to ibrutinib's pharmacology due to its structural similarity with A419259, a HCK inhibitor with established activity in murine tumor models.[16] Indeed both ibrutinib and A419259 were developed based on the 4-amino-5,7-substituted pyrrolopyrimidine scaffold of the classical SRC-family inhibitor: PP1.[26] To create a model for how ibrutinib might bind to HCK we performed a molecular docking studies of ibrutinib into the co-crystal structure of HCK with A419259 (RK-20449) (PDB 3VS3)[27] (Figure 6A). As expected, the docking study predicts that ibrutinib recognizes the ATP-binding pocket of HCK with an almost identical pose as A419259 with a calculated affinity energy (ΔG) of -10.5 kcal/mol. Similar to A419259, ibrutinib's 4-amino group, forms a H-bond to the carbonyl groups of the gatekeeper residue Thr^{333} (Thr^{338} based on c-SRC numbering)[16] and also with Glu^{334} of HCK; its 3-nitrogen atom, as an H-bond acceptor, interacts with the backbone amino group of Met^{336} of HCK (Figure 6A). The 4-phenoxyphenyl substituent at 5-postion of ibrutinib, which is also identical to the 5-substituent of A419259, extends into the inner ATP-hydrophobic pocket of HCK. The pyrrolidine group at the 7-position of ibrutinib,

the only distinctive substituent related to A419259, is predicted to interact with Ala^{390}, Asn^{391} or Asp^{404} of HCK, whereas the 7-substituent of A419259 protrudes outward the ATP-pocket and interacts with Asp^{348} (Figure 6A).

To confirm HCK target engagement in cells by ibrutinib, we synthesized a biotin modified version of ibrutinib. For comparative purposes we also prepared a biotin-modifed version of CC-292, a pyrimidine-based covalent BTK inhibitor.[28] Both ibrutinib and CC-292 use an acrylamide-moeity to form a covalent bond to Cys^{481} and are potent kinase inhibitors of BTK (reported apparent IC_{50} $\leq$0.5 nM).[11,28] Ibrutinib reversibly inhibits the kinase activity of HCK with an IC_{50} of 3.7 nM, while CC-292 is a very weak HCK inhibitor with an IC50 of 14.6 μM which is well above the observed physiological concentrations of this drug.[11,28] As expected, biotinylated ibrutinib and CC-292 pulled down BTK in mutated MYD88 expressing BCWM.1, MWCL-1 and TMD-8 cells demonstrating their ability to directly bind to BTK (Figure 6B). Biotinylated ibrutinib, but not CC-292 pulled down HCK in MYD88 mutated BCWM.1, MWCL-1 and TMD-8 cells thereby confirming binding of ibrutinib to HCK (Figure 6B).

To confirm target engagement in living cells, we performed KiNativ profiling where the ability of inhibitors to protect kinases from subsequent labeling with a reactive ATP-biotin probe is determined.[29] Living cells were treated with either ibrutinib, CC-292 or A419259, followed by lysis treatment with ATP-biotin and western blotting for BTK, HCK and other SRC family kinases. Consistent with the biochemical kinase assays, Ibrutinib and A419259, but not CC-292 blocked ATP binding to HCK in a dose-dependent manner, while ibrutinib and CC-292 but not A419259 blocked ATP binding to BTK in BCWM.1 WM cells. Consistent with its known activity, A419259 also blocked ATP binding to the SRC family members SRC and LYN. Conversely, ibrutinib and CC-292 did not block ATP binding to either SRC or LYN (Figure 6C).

HCK activity is blocked by ibrutinib and impacts survival of MYD88 mutated WM cells.

To assess the impact of ibrutinib and A419259 on HCK related activity in MYD88 mutated WM and ABC DLBCL tumor cells, we performed PhosFlow studies and assessed changes in HCK activation (Tyr^{411}). We also evaluated tumor cell viability by the CellTiter-Glo® Luminescent cell viability assay, and apoptosis by propidium iodide and Annexin V staining to determine if HCK inhibition contributed to WM cell death. We observed that ibrutinib, and even more so A419259, reduced HCK Tyr^{411} phosphorylation in MYD88 L265P expressing WM and ABC-DLBCL cell lines, as well as primary WM LPC. In contrast, CC-292 had little or no impact on HCK Tyr^{411} phosphorylation (Figure 7A). Decreased dose-dependent viability was also observed for ibrutinib and more so for A419259 that was more pronounced in mutated MYD88 versus $MYD88^{WT}$ cells (Figure 7B). In contrast, the BTK inhibitor CC-292 that lacks HCK kinase inhibition showed higher EC_{50} (>1 log-fold) for the mutated MYD88 cell lines, with the exception of OCI-Ly3 cells that carry a NF-κB activating CARD11 mutation (Figure 7B).[5] Increased apoptotic changes were also observed in the mutated MYD88 cell lines and primary WM cells that showed decreased viability following ibrutinib, and more so A419259. In contrast, CC-292 had little or no impact on apoptosis in mutated MYD88 cells (Figure 7C). In as well, we observed little or no apoptotic activity for ibrutinib, A419259 or CC-292 apoptosis in $MYD88^{WT}$ cell lines or healthy donor B-cells (data not shown). To investigate whether ibrutinib or A419259 induced killing of WM cells was a consequence of BTK and/or HCK inhibition, we transduced $MYD88^{L265P}$ expressing BCWM.1 WM cells with a lentiviral control vector or vectors expressing wild-type BTK; BTK with a mutation of the cysteine required for irreversible inhibition (BTK^{C481S}); wild-type HCK; or HCK with the gatekeeper mutation Thr^{333} (Thr^{338} based on c-SRC numbering).[16] Transduction of BCWM.1 WM cells with the BTK cysteine mutant (BTK^{C481S}) but not the vector control or wild-type BTK resulted in decreased ibrutinib and CC-292 mediated killing of BCWM.1 WM cells (<1 log-fold shift) (Figure 7D). In contrast, treatment with HCK

inhibitor A419259 showed no survival change versus vector control transduced cells (Figure 7D).

Transduction of BCWM.1 WM cells with the HCK gatekeeper mutant (HCKT333M; HCKT338M based on c-SRC numbering[16]) resulted in an >2 log-fold decrease in both ibrutinib and A419259 mediated tumor cell killing. Over-expression of wild-type HCK also resulted in one log-fold decrease in both ibrutinib and A419259 mediated mediated tumor cell killing when compared to control vector transduced BCWM.1 WM cells (Figure 7D). No substantial change in tumor cell killing following CC-292 treatment was observed in BCWM.1 cells transduced to express HCK^{T333M} or wild-type HCK (Figure 7D).

Discussion

We sought to clarify the contribution of non-BTK target(s) to the activity of ibrutinib in MYD88 mutated diseases such as WM. We focused this study on HCK, a member of the SRC family of kinases. HCK is over-expressed at early stages of B-cell development, and its transcriptional regulation is suppressed with terminal B-cell differentiation.[30,31] Using gene expression profiling, Guttierez et al[12] previously reported that HCK was highly over-expressed in malignant LPC taken from WM patients, though the genetic basis for this observation remained unclear. In this study, we observed that HCK was highly expressed in MYD88 mutated primary WM cells, WM and ABC-DLBCL cell lines, but was absent or expressed at low levels in healthy donor B-cells, as well as $MYD88^{WT}$ cell lines. Furthermore, we observed that over-expression of the $MYD88^{L265P}$ protein itself markedly induced HCK transcription across multiple B-cell lines, including both MYD88 mutated and wild-type cell lines. It is not likely that HCK transcription was triggered by MYD88 triggered IL6, since exogenous treatment of MYD88 mutated WM cells with IL6 or an IL6 antibody did not directly impact HCK transcription. In addition CXCR4 mutations that are found in up to 40% of WM patients neither impacted HCK transcription or activation in primary WM cells, nor did we observe

HCK transactivation in previous studies with MYD88 mutated BCWM.1 and MWCL-1 cells that were transduced with CXCR4 WHIM mutated receptors and stimulated with CXCL12 (unpublished observations).[32,33] Our findings therefore provide a genomic explanation for HCK over-expression in WM, and suggest that mutated MYD88 enforces high transcription levels of HCK. NF-kB, AP-1, and CREB binding sites are present on the promoter of HCK, and their transactivation is known to be triggered by wild-type MYD88 in response to TLR stimulation.[32,33,34] Studies to delineate the precise signaling cascade(s) by which mutated MYD88 transduces HCK are therefore needed, though the constitutive activation of NF-kB by mutated MYD88 is a strong suspect in WM and ABC DLBCL cells, as well as AP-1 in ABC DLBCL.[1,5,35] The B-cell receptor (BCR) and other pro-survival pathways may also contribute to HCK activation and warrant further investigation.

The findings also suggest an important role for IL6 in triggering HCK activity in WM, and possibly other MYD88 mutated diseases. We show that both IL6 and IL6R are highly expressed in WM disease, and that MYD88 L265P itself induces IL6 transcription. Ngo et al[5] showed that HCK and IL6 were among 285 genes whose transcription was down-regulated upon knockdown of MYD88 in HBL-1 ABC-DLBCL cells that express L265P as a heterozygous mutation. The role of IL6 as an activator of pHCK through IL6R/IL6ST has previously been reported, and appears dependent on an acidic domain (amino acids 771-811) of IL6ST.[13,14] IL6 is highly transcribed in WM and ABC-DLBCL tumors.[12,36,37] IL6 is also secreted by the bone marrow microenvironment in response to WM cell adhesion.[15] We show in these studies that HCK is hyper-activated in mutated MYD88 primary WM cells, as well as WM and ABC-DLBCL cell lines, and that exogenous IL6 induced its activation while knockdown of IL6ST attenuated HCK activation. HCK was also found to induce PI3K/AKT, MAPK/ERK, and BTK signaling, providing for the first time evidence that mutated MYD88 can trigger pro-survival signaling beyond its known activation of NFKB by eliciting HCK transcription and activation. The transactivation of BTK by HCK is also noteworthy. Cheng et al previously

described showed that BTK could bind to HCK through SH3 mediated interactions. In previous work, we described that the activated form BTK was complexed with MYD88 in MYD88 mutated cells, though the mechanism for BTK activation in this context remained unclear. Our findings offer a mechanistic explanation for BTK activation in MYD88 mutated WM and ABC DLCBL cells.

A key finding of this study was the recognition of HCK as a novel therapeutic target for WM, and possibly other mutated MYD88 diseases. Kinase selectivity profiling had previously implicated HCK as a potential target of ibrutinib with an IC_{50} of 3.7 nM, a dose level close to the IC_{50} of BTK (0.5 nM) and well within the pharmacologically achievable levels of ibrutinib.[11,38] We provide definitive evidence in this report that HCK is a target of ibrutinib using docking models, direct pull-down experiments with biotinylated ibrutinib, cellular target engagement and cellular rescue with inhibitor-resistant mutant proteins. We also observed that treatment of mutated MYD88 WM and ABC-DLBCL cells with ibrutinib or a preclinical HCK inhibitor (A419259) attenuated HCK activation, while over-expression of wild-type HCK and more so HCK bearing a mutated gatekeeper (HCK^{T333M}; HCK^{T338M} based on c-SRC numbering)[16] reduced the activity of both of these compounds in MYD88 mutated cells. The attenuation of MYD88 directed HCK activity may provide mechanistic insights into the high response activity observed in MYD88 mutated WM and ABC-DLBCL patients undergoing ibrutinib therapy.[4,10] It also remains possible that mutations in the gatekeeper site of HCK could contribute to ibrutinib resistance, akin to that observed with BTK^{C481S} mutations in CLL patients, and warrant examination.[39] Finally, the potential to develop more potent HCK inhibitors is suggested by these findings. While ibrutinib suppressed HCK activity, higher levels of HCK suppression were observed with A419259, and were associated with greater levels of apoptosis in MYD88 mutated WM and ABC-DLBCL cells. Several scaffolds for targeted HCK inhibition are in development based on prior work implicating HCK in the pathogenesis of several solid and hematological malignancies, as well as productive HIV infection.[40,41] In

addition to inhibiting other SRC family members, dasatinib also shows potent inhibition of HCK and may be active in diseases dependent on mutated MYD88.[42]

In summary, our findings suggest that HCK is a downstream target of mutated MYD88, is activated by IL6, and triggers pro-survival signaling including PI3K/AKT, MAPK/ERK and BTK in MYD88 mutated cells. HCK is also a highly relevant target of ibrutinib, and represents a novel focus for therapeutic development in WM, and possibly other diseases driven by mutated MYD88.

Acknowledgements

The authors gratefully acknowledge the generous support of the Peter Bing M.D., the International Waldenstrom's Macroglobulinemia Foundation, the Leukemia and Lymphoma Society, the Edward and Linda Nelson Fund for WM Research, the Bauman Family Trust, the Tannenhauser Family Foundation, and the WM patients who provided samples for these studies. The authors also acknowledge the kind gift of Dr. Thomas Smithgall for providing the HCK inhibitor resistant mutant construct used in these studies.

Author Contributions

GY, SB, TL, NG and SPT conceived and designed the experiments. GY and SPT wrote the manuscript. GY, ZRH and SPT performed the data analysis. XL, NT performed PCR-based sequencing studies. GY, XL, JC performed transduction experiments. GY and JC performed PhosFlow studies. TL, SB, and NG performed docking studies. LX, XL, and CJP prepared samples. SPT, JB, and JJC provided patient care, obtained consent and samples. WZ, XZ, SL provided biotinylated Ibrutinib. PC provided BTK-C481S and HCK-T333M vectors for transduction experiments.

Conflict of Interest Disclosures

ST and JB have received research funding, consulting fees, and/or honoraria from Pharmacyclics Inc., and Janssen Oncology Inc.

References

1. Treon SP, Xu L, Yang G, Zhou Y, Liu X, Cao Y, et al: MYD88 L265P somatic mutation in Waldenstrom's macroglobulinemia. N Engl J Med 2012; 367(15):826-33.2.
2. Xu L, Hunter Z, Yang G, Zhou Y, Cao Y, Liu X, et al. MYD88 L265P in Waldenstrom macroglobulinemia, immunoglobulin M monoclonal gammopathy, and other B-cell lymphoproliferative disorders using conventional and quantitative allele-specific polymerase chain reaction. Blood 2013; 121:2051-8.
3. Varettoni M, Arcaini L, Zibellini S, Boveri E, Rattotti S, Riboni R, et al. Prevalence and clinical significance of the MYD88 L265P somatic mutation in Waldenstrom macroglobulinemia, and related lymphoid neoplasms. Blood 2013; 121: 2522-8.
4. Treon SP, Xu L, Hunter ZR. MYD88 mutations and response to ibrutinib in Waldenstrom's Macroglobulinemia. N Engl J Med 2015; 373:584-6.
5. Ngo VN, Young RM, Schmitz R, Jhavar S, Xiao W, Lim KH, et al: Oncogenically active MYD88 mutations in human lymphoma. Nature 2011, 470:115-9.
6. Bohers E, Mareschal S, Bouzelfen A, Marchand V, Ruminy P, Maingonnat C, et al. Targetable activating mutations are very frequent in GCB and ABC Diffuse Large B-cell Lymphoma. Genes, Chromosomes, Cancer 2014; 53:144-153.
7. Yang G, Zhou Y, Liu X, Xu L, Cao Y, Manning RJ, et al. A mutation in MYD88 (L265P) supports the survival of lymphoplasmacytic cells by activation of Bruton tyrosine kinase in Waldenstrom macroglobulinemia. Blood 2013; 122:1222-32.
8. Treon SP, Tripsas CK, Meid K, Warren D, Varma G, Green R, et al. Ibrutinib in previously treated Waldenstrom's Macroglobulinemia. N Engl J Med 2015; 372:1430-40.

9. Treon SP, Xu L, Hunter ZR. MYD88 mutations and response to ibrutinib in Waldenström's Macroglobulinemia. N Engl J Med 2015; 373:584-6.
10. Wilson WH, Young RM, Schmitz R, Yang Y, Pittaluga S, Wright G, et al. Targeting B cell receptor signaling with ibrutinib in diffuse large B cell lymphoma. Nat Med 2015; 21:922-6.
11. Honigberg LA, Smith AM, Sirisawad M, Verner E, Loury D, Chang B, et al. The Bruton tyrosine kinase inhibitor PCI-32765 blocks B-cell activation and is efficacious in models of autoimmune disease and B-cell malignancy. Proc Natl Acad Sci USA 2010; 107:13075-80.
12. Gutiérrez NC, Ocio EM, de las Rivas J, Maiso P, Delgado M, Ferminan E, et al. Gene expression profiling of B lymphocytes and plasma cells from Waldenström's macroglobulinemia: comparison with expression patterns of the same cell counterparts from chronic lymphocytic leukemia, multiple myeloma and normal individuals. Leukemia 2007; 21:541–549.
13. Hallek M, Neumann C, Schäffer M, Danhauser-Riedl S, von Bubnoff N, de Vos G, et al. Signal transduction of interleukin-6 involves tyrosine phosphorylation of multiple cytosolic proteins and activation of Src-family kinases Fyn, Hck, and Lyn in multiple myeloma cell lines. Exp Hematol 1997; 25:1367-77.
14. Schaeffer M, Schneiderbauer M, Weidler S, Tavares R, Warmuth W, de Vos G, et al. Signaling through a novel domain of gp130 mediates cell proliferation and activation of Hck and Erk kinases. Mol Cell Biol 2001; 21:8068-81.
15. Leleu X, Jia X, Runnels J, Ngo HT, Moreau AS, Farag M, et al. The Akt pathway regulates survival and homing in Waldenstrom macroglobulinemia. Blood 2007; 110:4417-26.
16. Pene-Dumitrescu T, Peterson LF, Donato NJ, Smithgall TE. An inhibitor-resistant mutant of HCK protects CML cells against the anti-proliferative and apoptotic effects of the broad-spectrum SRC family kinase inhibitor A-419259. Oncogene 2008; 27:7055-69.

17. Sanner MF, Olson AJ, Spehner JC. Reduced surface: an efficient way to compute molecular surfaces. Biopolymers 1996; 38: 305-20.
18. Trott O, Olson AJ. AutoDock Vina: improving the speed and accuracy of docking with a new scoring function, efficient optimization, and multithreading. J Comput Chem 2010; 31: 455-61.
19. O'Boyle NM, Banck M, James CA, Morley C, Vandermeersch T, Hutchison GR. Open Babel: An open chemical toolbox. J Cheminform 2011; 3:33.
20. Sahota SS1, Babbage G, Weston-Bell NJ. CD27 in defining memory B-cell origins in Waldenström's Macroglobulinemia. Clin. Lymphoma Myeloma 2009; 9:33-5.
21. Janz S. Waldenström Macroglobulinemia: Clinical and Immunological Aspects, Natural History, Cell of Origin, and Emerging Mouse Models. ISRN Hematol. 2013; 2013: 815325.
22. Cheng G, Ye ZS, Baltimore D. Binding of Bruton's tyrosine kinase to Fyn, Lyn, or Hck through a Src homology 3 domain-mediated interaction. Proc Natl Acad Sci USA1994; 91(17):8152-5.
23. Hong H, Kitaura J, Xiao W, Horejsi V, Ra C, Lowell CA, et al. The Src family kinase Hck regulates mast cell activation by suppressing an inhibitory Src family kinase Lyn. Blood 2007; 110:2511-9.
24. Suh HS, Kim MO, Lee SC. Inhibition of granulocyte-macrophage colony-stimulating factor signaling and microglial proliferation by anti-CD45RO: role of Hck tyrosine kinase and phosphatidylinositol 3-kinase/Akt. J Immunol 2005; 174:2712-9.
25. Pecquet C, Nyga R, Penard-Lacronique V, Smithgail TE, Murakami H, Regnier A, et al. The Src tyrosine kinase Hck is required for Tel-Abl- but not for Tel-Jak2-induced cell transformation. Oncogene 2007; 26:1577–85.
26. Hanke JH, Gardner JP, Dow RL, Changelian PS, Brisette WH, Weringer EJ, et al. Discovery of a novel, potent, and Src family-selective tyrosine kinase inhibitor. Study of Lck- and FynT-dependent T cell activation. J Biol Chem 1996; 271: 695-701.

27. Saito Y, Yuki H, Kuratani M, Hashizume Y, Takagi S, Tanaka A, et al. A pyrrolo-pyrimidine derivative targets human primary AML stem cells in vivo. Sci Transl Med. 2013; 5:181ra52.
28. Evans EK, Tester R, Aslanian S, Karp R, Sheets M, Labenski MT, et al. Inhibition of Btk with CC-292 provides early pharmacodynamic assessment of activity in mice and humans. J Pharmacol Exp Ther 2013; 346:219-28.
29. Patricelli MP, Nomanbhoy TK, Wu J, Brown H, Zhou D, Zhang J, et al. In situ kinase profiling reveals functionally relevant properties of native kinases. Chem Biol. 2011; 18:699-710.
30. Taguchi T, Kiyokawa N, Sato N, Saito M, Fujimoto J. Characteristic expression of Hck in human B-cell precursors. Exp Hematol 2000; 28:55-64.
31. Jourdan M, Caraux A, Caron G, Robert N, Fiol G, Reme T, et al. Characterization of a transitional preplasmablast population in the process of human B cell to plasma cell differentiation. J Immunol 2011; 187:3931-41.
32. Cao Y, Hunter ZR, Liu X, Xu L, Yang G, Chen J, et al. The WHIM-like CXCR4^{S338X} somatic mutation activates AKT and ERK, and promotes resistance to ibrutinib and other agents used in the treatment of Waldenstrom's Macroglobulinemia. Leukemia 2015; 29:169-76.
33. Cao Y, Hunter ZR, Liu X, Xu L, Yang G, Chen J, et al. CXCR4 WHIM-like frameshift and nonsense mutations promote ibrutinib resistance but do not supplant MYD88 L265P directed survival signaling in Waldenstrom Macroglobulinemia cells. Br J Haematol. 2015; 168:701-7.
34. Gay NJ, Symmons MF, Gangloff M, Bryant CE. Assembly and localization of Toll-like receptor signalling complexes. Nat Reviews Immunol. 2014; 14:546-58.
35. Messeguer X, Escudero R, Farré D, Núñez O, Martínez J, Albà MM. PROMO: detection of known transcription regulatory elements using species-tailored searches. Bioinformatics. 2002;18(2):333-4.
36. Farré D, Roset R, Huerta M, Adsuara JE, Roselló L, Albà MM, Messeguer X. Identification of patterns in biological sequences at the ALGGEN server: PROMO and MALGEN. Nucleic Acids Res. 2003; 31(13):3651-3.

37. Juilland M, Gonzalez M, Erdmann T, Banz Y, Jevnikar Z, Hailfinger S, et al. CARMA1- and MYD88-dependent activation of Jun/ATF-type AP-1 complexes is a hallmark of ABC diffuse large B-cell lymphomas. Blood 2016; an 8. pii: blood-2015-07-655647. [Epub ahead of print]
38. Chng WJ, Schop RF, Price-Troska T, Ghobrial I, Kay N, Jelinek DF, et al. Gene-expression profiling of Waldenstrom macroglobulinemia reveals a phenotype more similar to chronic lymphocytic leukemia than multiple myeloma. Blood 2006; 108(8): 2755-63.
39. Lam LT, Wright G, Davis RE, Lenz G, Farinha P, Dang L, et al. Cooperative signaling through the signal transducer and activator of transcription 3 and nuclear factor-kappa B pathways in subtypes of diffuse large B-cell lymphoma. Blood 2008; 111:3701-13.
40. Advani R, Buggy JJ, Sharman JP, Smith SM, Boyd TE, Grant B, et al. Bruton tyrosine kinase inhibitor ibrutinib (PCI-32765) has significant activity in patients with relapsed/refractor B-cell malignancies. J Clin Oncol 2013; 31:88-94.
41. Woyach JA, Furman RR, Liu TM, Ozer HG, Zapatka M, Ruppert AS, et al. Resistance mechanisms for the Bruton's tyrosine kinase inhibitor ibrutinib. N Engl J Med 2014; 370:2286-94.
42. Musumeci F, Schenone S, Brullo C, Desoqus A, Botta L, Tinton C. HCK inhibitors as potential therapeutic agents in cancer and HIV infection. Curr Med Chem 2015; 22:1540-64.
43. Poh AR, O'Donoghue R JJ, Ernst M. Hematopoeitic cell kinase (HCK) as a therapeutic target in immune and cancer cells. Oncotarget 2015; 6:15752-71.
44. Yang C, Lu P, Lee FY, Chadburn A, Barrientos JC, Leonard JP, et al. Tyrosine kinase inhibition in diffuse large B-cell lymphoma: molecular basis for antitumor activity and drug resistance of dasatinib. Leukemia 2008; 22:1755-66.

Legends

Figure 1. HCK transcription is driven by mutated MYD88.

(A) HCK transcript levels in MYD88 mutated WM (BCWM.1, MWCL-1) and ABC DLBCL (TMD-8, HBL-1, OCI-Ly3, SU-DHL2) cells, and MYD88 wild-type (OCI-Ly7 and OCI-Ly19 GCB DLBCL, Ramos Burkitt, MM1.S and RPMI-8226 myeloma) cells by quantitative RT-PCR. **(B)** HCK transcription using TaqMan® Gene Expression Assay in primary lymphoplasmacytic cells ($CD19^+$) from MYD88 L265P expressing WM patients, and healthy donor derived non-memory ($CD19^+CD27^-$) and memory ($CD19^+CD27^+$) B-cells. $p<0.01$ for comparison of WM LPC versus either healthy donor non-memory or memory B-cells. **(C)** Fold change in HCK transcription following lentiviral transduction with vector control, Flag-tagged MYD88 L265P or MYD88 wild-type protein in cell lines expressing mutated or wild-type MYD88. At the bottom of the Figure 1C, total Flag-tagged MYD88 L265P or wild-type protein levels are shown for all transduced cell lines to demonstrate relative translation efficiency for MYD88 L265P and wild-type vectors, as well as GAPDH protein levels as protein loading controls.

Figure 2. IL6 but not IL6R transcription is induced by mutated MYD88.

Expression of IL6 **(A)** and IL6R **(B)** transcripts using TaqMan® Gene Expression Assays in MYD88 mutated and MYD88 wild-type (WT) cell lines. IL6 **(C)** and IL6R **(D)** transcript levels were also determined by TaqMan® Gene Expression Assays in primary lymphoplasmacytic cells ($CD19^+$) from MYD88 L265P expressing WM patients, and healthy donor derived non-memory ($CD19^+CD27^-$) and memory ($CD19^+CD27^+$) B-cells. $p<0.01$ for comparison of IL6 or IL6R transcript levels in WM LPC versus either healthy donor non-memory or memory B-cells. IL6 **(E)** and IL6R **(F)** transcription following over-expression of MYD88 L265P or wild-type protein in cell lines expressing mutated or wild-type MYD88. Total Flag-tagged

MYD88 L265P or wild-type protein, as well as GAPDH protein levels determined by immunoblotting are shown for all transduced cell lines in Figure 1C.

Figure 3. HCK is hyperactive in MYD88 mutated cells, and its activation is triggered by IL6.

(A) Results of PhosFlow analysis for phosphorylated HCK ($pHCK^{Tyr411}$) in MYD88 mutated WM (BCWM.1, MWCL-1) and ABC DLBCL (TMD-8, OCI-Ly3) cells; MYD88 wild-type GCB DLBCL (OCI-Ly7, OCI-Ly19), Ramos Burkitt, and RPMI-8226 myeloma cells. **(B)** Results of PhosFlow analysis for $pHCK^{Tyr411}$ in primary lymphoplasmacytic cells ($CD20^{+}$) from 3 representative MYD88 L265P expressing WM patients, as well as non-memory ($CD20^{+}CD27^{-}$) and memory ($CD20^{+}CD27^{+}$) B-cells from healthy donors. Percentage of cells gating for $pHCK^{Tyr411}$ expression are shown in A and B. Histogram depicts the results of $pHCK^{Tyr411}$ expression in LPC derived from 20 WM patients, as well as non-memory and memory B-cells from 5 healthy donors. $p<0.01$ for comparison of p-HCK expression in WM LPC versus either healthy donor non-memory or memory B-cells. **(C)** $pHCK^{Tyr411}$ expression in the presence or absence of IL6 (1 ng/mL) for 5 minutes in MYD88 mutated (BCWM.1, MWCL-1, TMD-8, HBL-1, OCI-Ly3) and MYD88 wild-type (OCI-Ly7, OCI-Ly19, Ramos, RPMI 8226) cell lines, as well as primary WM lymphoplasmacytic cells. Peak $pHCK^{Tyr411}$ activation was determined by PhosFlow analysis after three MYD88 mutated cell lines were cultured with IL6 (1 ng/mL) for 2, 5, and 15 minutes. **(D)** PhosFlow analysis of $pHCK^{Tyr411}$ in BCWM.1 cells transduced with scrambled control vector or IL6ST knockdown vector (shRNA2) in the presence or absence of 1 ng/mL of IL6.

Figure 4. HCK is a determinant of survival in MYD88 mutated cells.

(A) HCK protein levels determined by western blot analysis and **(B)** survival determined by AlamarBlue® cell viability assay over a 9 day evaluation period in MYD88 mutated BCWM.1 and MWCL-1 WM cells, and TMD-8 and HBL-1 ABC DLBCL cells following transduction with inducible HCK knockdown (shRNA1,

shRNA2) or scrambled control vectors. Mean of two independent experiments is depicted for time points.

Figure 5. HCK triggers pro-survival signaling in MYD88 mutated WM cells.

(A) PhosFlow analysis for pHCK^{Tyr411}, pBTK, pAKT, and pERK in scramble control vector or HCK transduced MYD88 mutated BCWM.1 and MWCL-1 cells. **(B)** Impact of HCK over-expression or **(C)** HCK knockdown on PI3K/AKT (PIK3R2, AKT), MAPK (PLCγ1, ERK1/2), BTK (BTK, PLCγ2), and IRAK4 signaling in BCWM.1 and MWCL-1 cells using antibodies to detect phospho-specific and total protein expression by immunoblotting. GAPDH protein levels were determined for control purposes in all experiments.

Figure 6. Ibrutinib binds to the ATP-binding pocket of HCK and blocks ATP binding.

(A) Docking model of the Ibrutinib (purple stick) aligned with the co-crystal structure of HCK (green ribbon)-A419259 (yellow stick). The hydrogen bonds between the aminopyrimidine moiety of Ibrutinib and the hinge region of HCK are indicated. Docking studies showed that ibrutinib bound to the ATP-binding pocket of HCK with calculated affinity energy (ΔG) of -10.5 kcal/mol. **(B)** Results from pull-down experiments using streptavidin beads (SVB) and biotinylated ibrutinib (IB-BTN) and CC-292 (CC-BTN) to detect BTK and HCK binding in MYD88 mutated BCWM.1, MWCL-1 and TMD-8 cells. **(C)** Results from kinase active-site inhibition assays utilizing an ATP-biotin (ATP-BTN) probe that was used to pull-down active kinases in presence of ibrutinib, CC-292, or A419259 in lysates from BCWM.1 WM cells.

Figure 7. HCK activity is blocked by ibrutinib and impacts survival of MYD88 mutated WM cells.

(A) PhosFlow analysis showing changes in $pHCK^{Tyr411}$ following treatment of MYD88 mutated WM (BCWM.1, MWCL-1) and ABC DLBCL (TMD-8, OCI-Ly3, HBL-1) cells and MYD88 mutated primary lymphoplasmacytic cells from 4 WM patients with 0.5 uM of A419259, ibrutinib or CC-292 for 30 minutes. **(B)** Dose dependent survival determined by CellTiter-Glo® Luminescent cell viability assay for mutated (BCWM.1, MWCL-1, TMD-8, HBL-1, OCI-LY3) and wild type (OCI-LY7, OCI-LY19, Ramos, RPMI 8226) MYD88 cells following treatment with ibrutinib, A419259 or CC-292 for 72 hours. **(C)** Apoptotic changes using propidium iodide (PI) and Annexin V (FITC-A) staining following treatment of mutated and wild type MYD88 cell lines, and primary lymphoplasmacytic cells from 3 WM patients with 0.5 uM of A419259, ibrutinib or CC-292 for 18 hours. DMSO denotes vehicle control only treated cells. Cell line results are from experiments performed in triplicate. Primary LPC data are from results obtained from 6 WM patients. (*) $p \leq 0.05$ and (**) $p \leq 0.01$ versus DMSO controls **(D)** Dose dependent tumor cell survival of MYD88 mutated BCWM.1 cells transduced with control vector or vectors expressing wild-type BTK (BTK WT); BTK expressing mutated site for ibrutinib binding (BTK C481S); wild-type HCK (HCK WT); or HCK expressing the gatekeeper mutation (HCK^{T333M}; HCK^{T338M} based on c-SRC numbering)[16] and treated with ibrutinib, A419259 or CC-292. Protein levels following transduction with control, wild-type or mutated BTK or HCK vectors are also shown at the bottom of Figure 7D.

Figure 1.

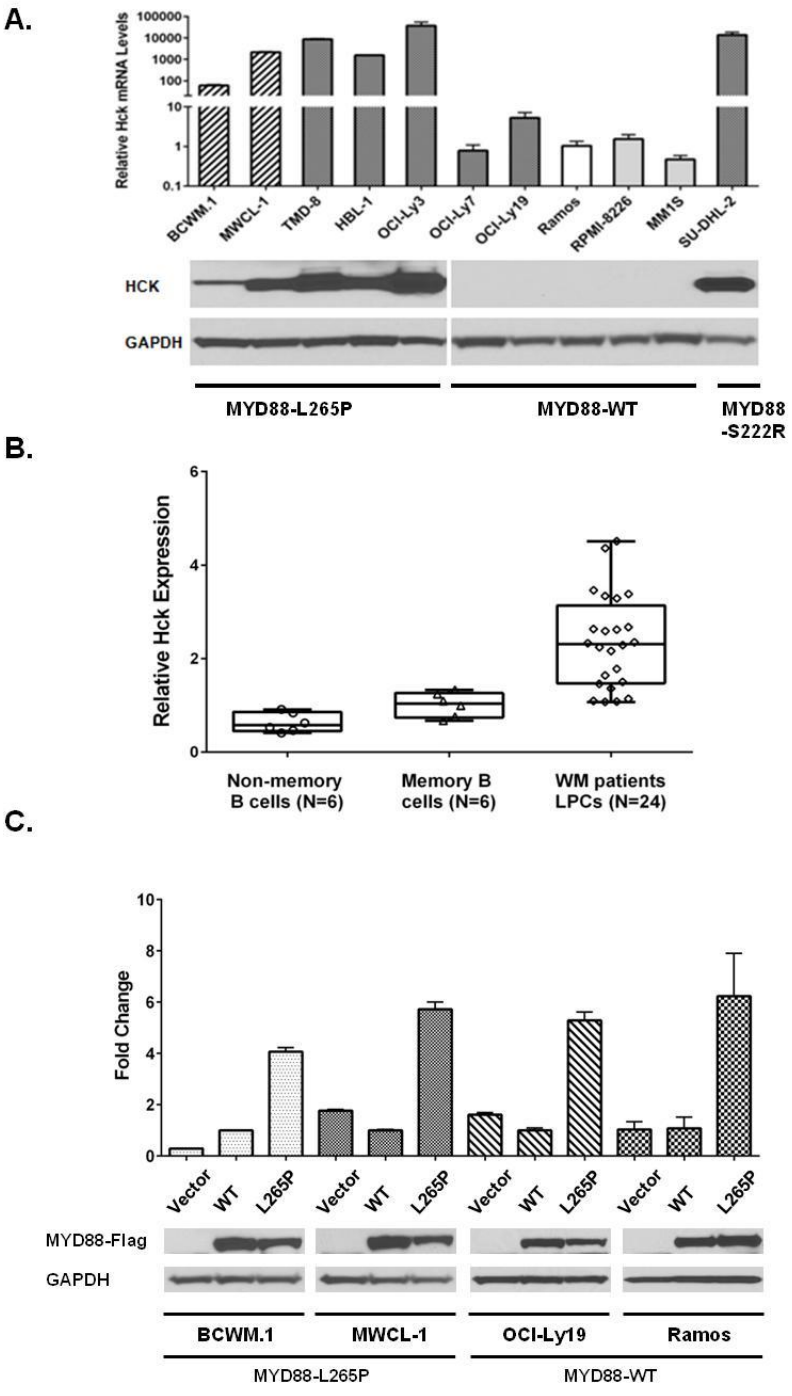
A.
Relative Hck mRNA Levels
100000
10000
1000
100
10
1
0.1
BCWM.1
MWCL-1
TMD-8
HBL-1
OCI-Ly3
OCI-Ly7
OCI-Ly19
Ramos
RPMI-8226
MM1S
SU-DHL-2
HCK
GAPDH
MYD88-L265P
MYD88-WT
MYD88 -S222R
B.
Relative Hck Expression
6
4
2
0
Non-memory B cells (N=6)
Memory B cells (N=6)
WM patients LPCs (N=24)
C.
Fold Change
10
8
6
4
2
0
Vector
WT
L265P
MYD88-Flag
GAPDH
BCWM.1
MWCL-1
OCI-Ly19
Ramos
MYD88-L265P
MYD88-WT

Figure 2.

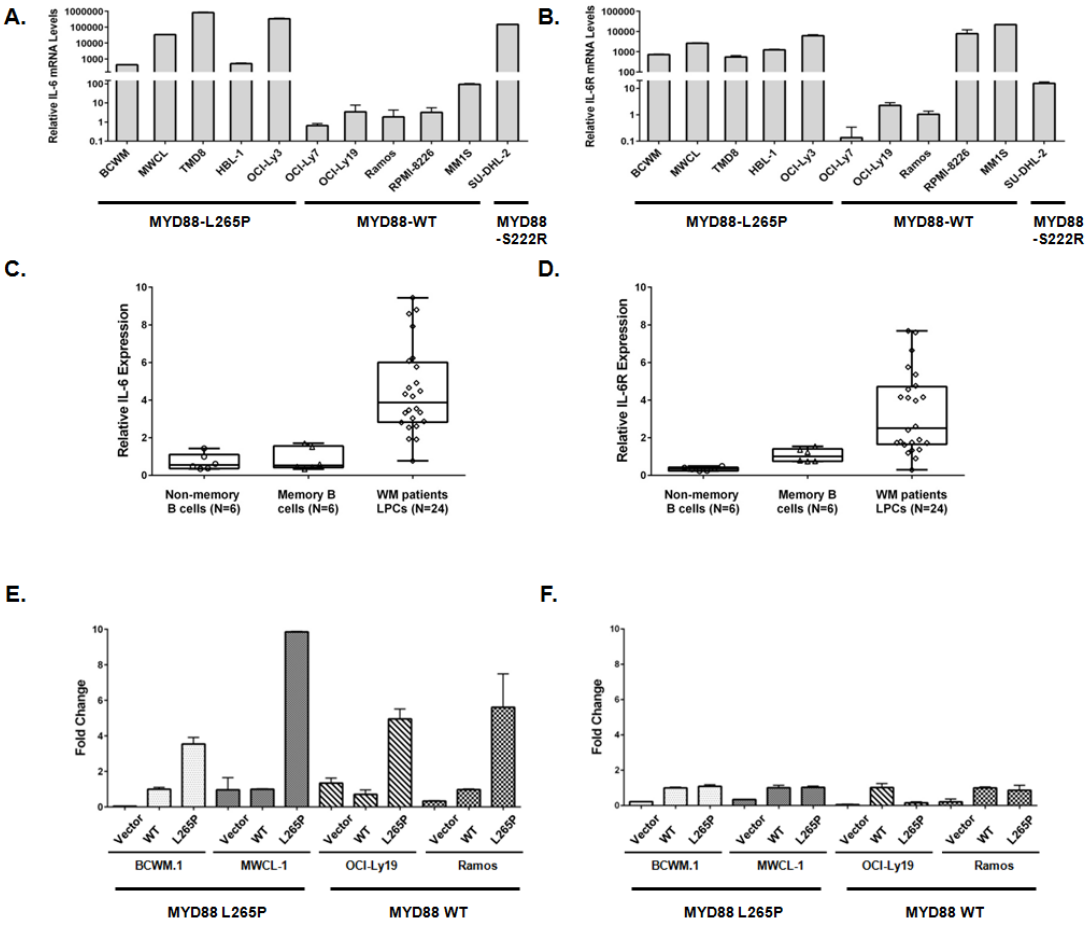
A.
Relative IL-6 mRNA Levels
BCWM
MWCL
TMD8
HBL-1
OCI-Ly3
OCI-Ly7
OCI-Ly19
Ramos
RPMI-8226
MM1S
SU-DHL-2
MYD88-L265P
MYD88-WT
MYD88 -S222R
B.
Relative IL-6R mRNA Levels
C.
Relative IL-6 Expression
Non-memory B cells (N=6)
Memory B cells (N=6)
WM patients LPCs (N=24)
D.
Relative IL-6R Expression
E.
Fold Change
Vector
WT
L265P
BCWM.1
MWCL-1
OCI-Ly19
Ramos
MYD88 L265P
MYD88 WT
F.

Figure 3.

A.

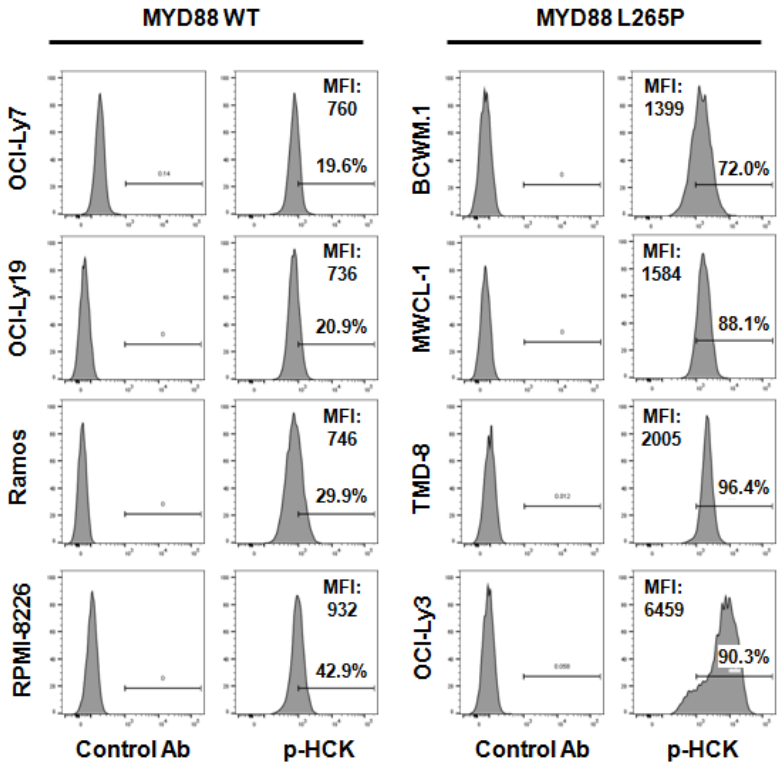
MYD88 WT
MYD88 L265P
OCI-Ly7
OCI-Ly19
Ramos
RPMI-8226
BCWM.1
MWCL-1
TMD-8
OCI-Ly3
MFI: 760
19.6%
MFI: 736
20.9%
MFI: 746
29.9%
MFI: 932
42.9%
MFI: 1399
72.0%
MFI: 1584
88.1%
MFI: 2005
96.4%
MFI: 6459
90.3%
Control Ab
p-HCK
Control Ab
p-HCK

B.

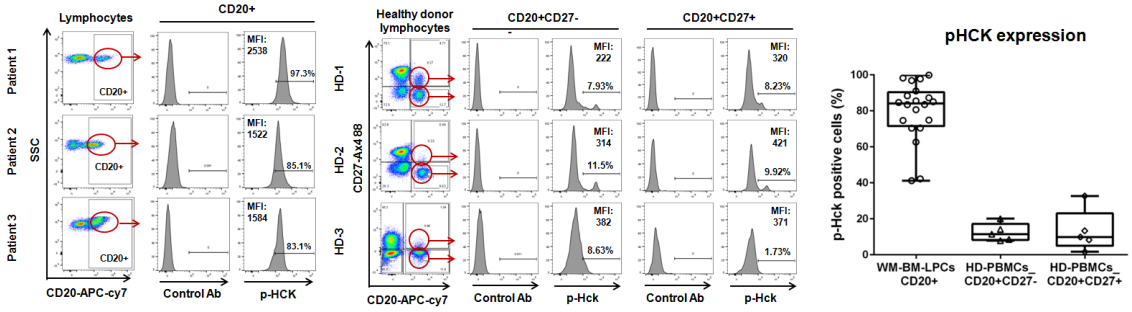
Lymphocytes
CD20+
Healthy donor lymphocytes
CD20+CD27-
CD20+CD27+
Patient 1
Patient 2
Patient 3
SSC
CD20+
MFI: 2538
97.3%
MFI: 1522
85.1%
MFI: 1584
83.1%
HD-1
HD-2
HD-3
CD27-Ax488
MFI: 222
7.93%
MFI: 314
11.5%
MFI: 382
8.63%
MFI: 320
8.23%
MFI: 421
9.92%
MFI: 371
1.73%
CD20-APC-cy7
Control Ab
p-HCK
CD20-APC-cy7
Control Ab
p-Hck
Control Ab
p-Hck
pHCK expression
p-Hck positive cells (%)
100
80
60
40
20
0
WM-BM-LPCs CD20+
HD-PBMCs_ CD20+CD27-
HD-PBMCs_ CD20+CD27+

C.

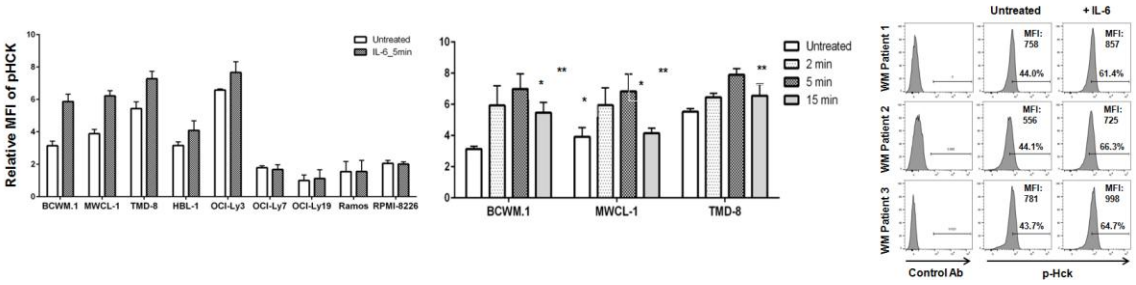
Relative MFI of pHCK
Untreated
IL-6_5min
BCWM.1
MWCL-1
TMD-8
HBL-1
OCI-Ly3
OCI-Ly7
OCI-Ly19
Ramos
RPMI-8226
Untreated
2 min
5 min
15 min
Untreated
+ IL-6
WM Patient 1
WM Patient 2
WM Patient 3
MFI: 758
MFI: 857
44.0%
61.4%
MFI: 556
MFI: 725
44.1%
66.3%
MFI: 781
MFI: 998
43.7%
64.7%
Control Ab
p-Hck

D.

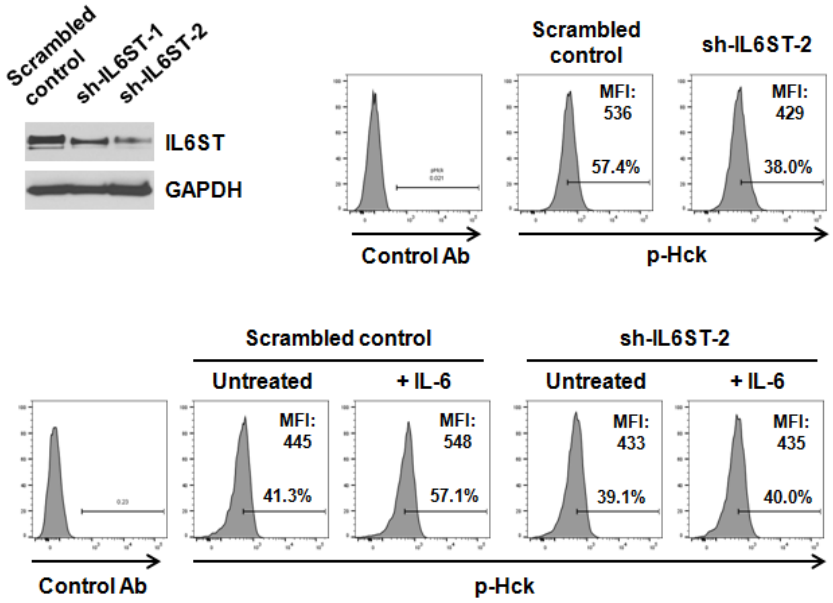
Scrambled control
sh-IL6ST-1
sh-IL6ST-2
IL6ST
GAPDH
Scrambled control
sh-IL6ST-2
MFI: 536
57.4%
MFI: 429
38.0%
Control Ab
p-Hck
Scrambled control
sh-IL6ST-2
Untreated
+ IL-6
Untreated
+ IL-6
MFI: 445
41.3%
MFI: 548
57.1%
MFI: 433
39.1%
MFI: 435
40.0%
Control Ab
p-Hck

Figure 4.

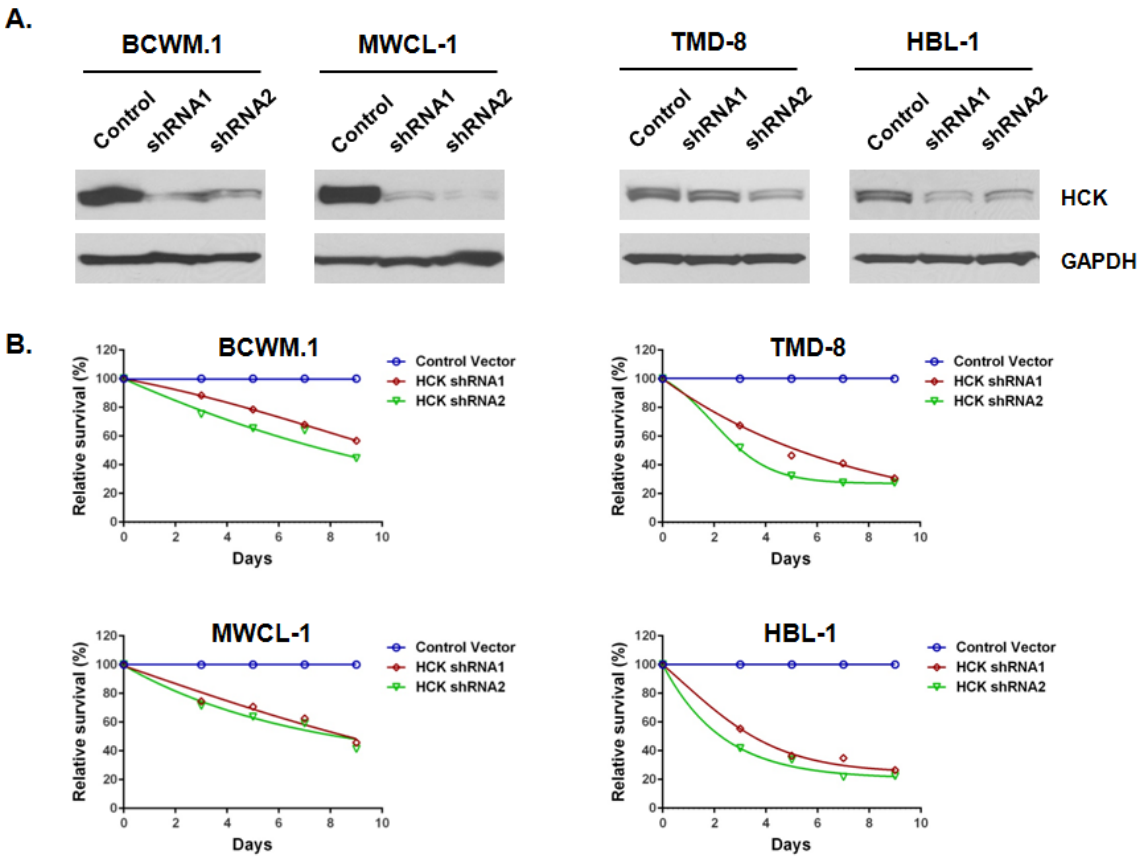
A.
BCWM.1
MWCL-1
TMD-8
HBL-1
Control
shRNA1
shRNA2
HCK
GAPDH
B.
BCWM.1
MWCL-1
TMD-8
HBL-1
Relative survival (%)
Days
Control Vector
HCK shRNA1
HCK shRNA2

Figure 5.

A.

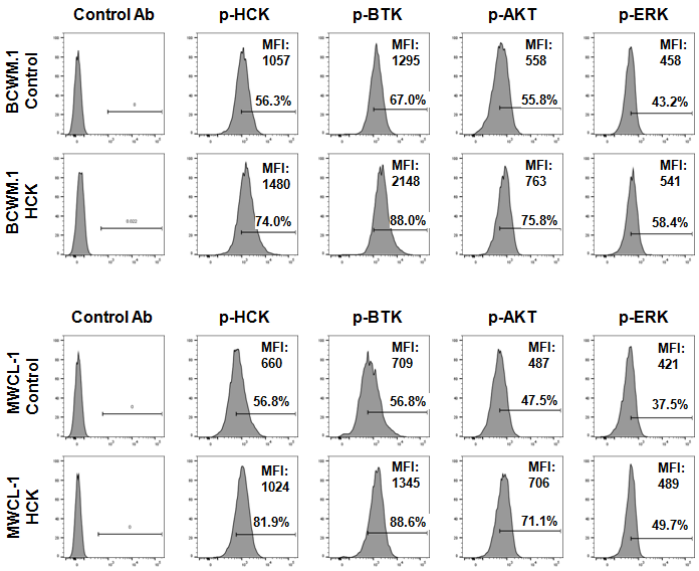
Control Ab
p-HCK
p-BTK
p-AKT
p-ERK
BCWM.1 Control
MFI: 1057
56.3%
MFI: 1295
67.0%
MFI: 558
55.8%
MFI: 458
43.2%
BCWM.1 HCK
MFI: 1480
74.0%
MFI: 2148
88.0%
MFI: 763
75.8%
MFI: 541
58.4%
Control Ab
p-HCK
p-BTK
p-AKT
p-ERK
MWCL-1 Control
MFI: 660
56.8%
MFI: 709
56.8%
MFI: 487
47.5%
MFI: 421
37.5%
MWCL-1 HCK
MFI: 1024
81.9%
MFI: 1345
88.6%
MFI: 706
71.1%
MFI: 489
49.7%

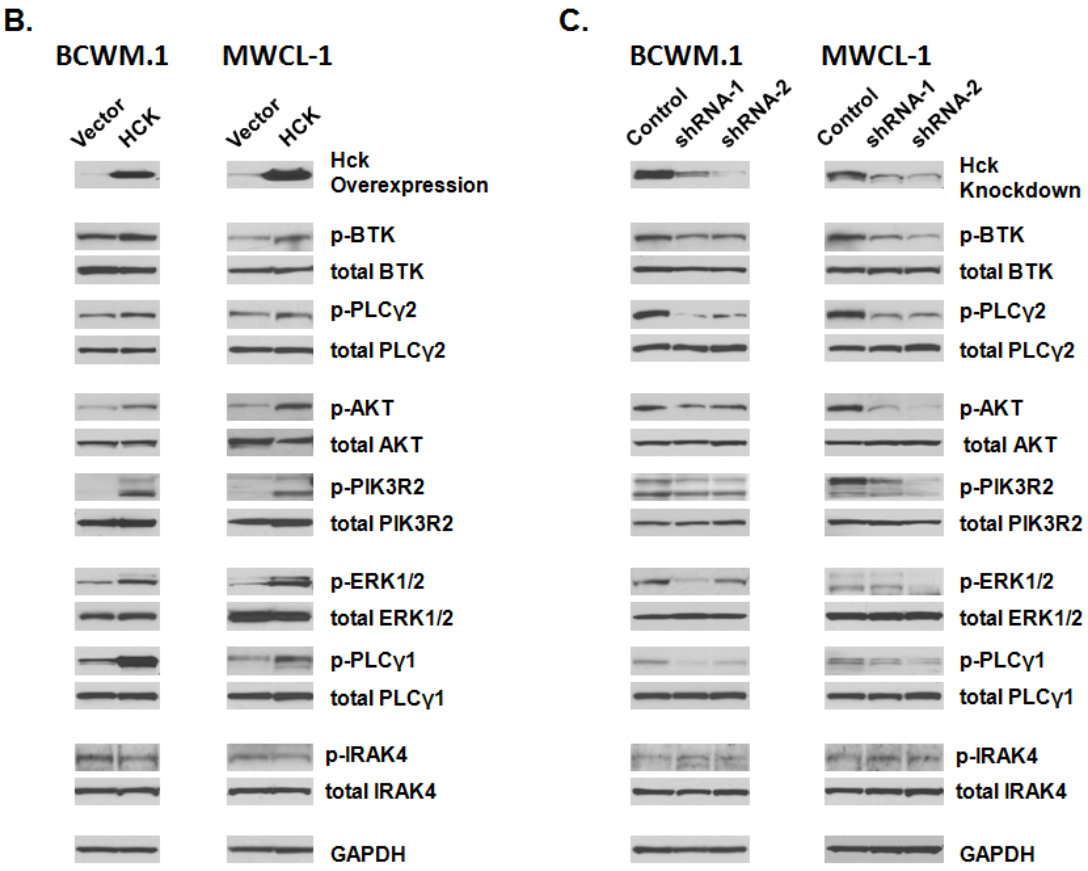
B.
BCWM.1
MWCL-1
Vector
HCK
Vector
HCK
Hck Overexpression
p-BTK
total BTK
p-PLCγ2
total PLCγ2
p-AKT
total AKT
p-PIK3R2
total PIK3R2
p-ERK1/2
total ERK1/2
p-PLCγ1
total PLCγ1
p-IRAK4
total IRAK4
GAPDH
C.
BCWM.1
MWCL-1
Control
shRNA-1
shRNA-2
Control
shRNA-1
shRNA-2
Hck Knockdown
p-BTK
total BTK
p-PLCγ2
total PLCγ2
p-AKT
total AKT
p-PIK3R2
total PIK3R2
p-ERK1/2
total ERK1/2
p-PLCγ1
total PLCγ1
p-IRAK4
total IRAK4
GAPDH

Figure 6.

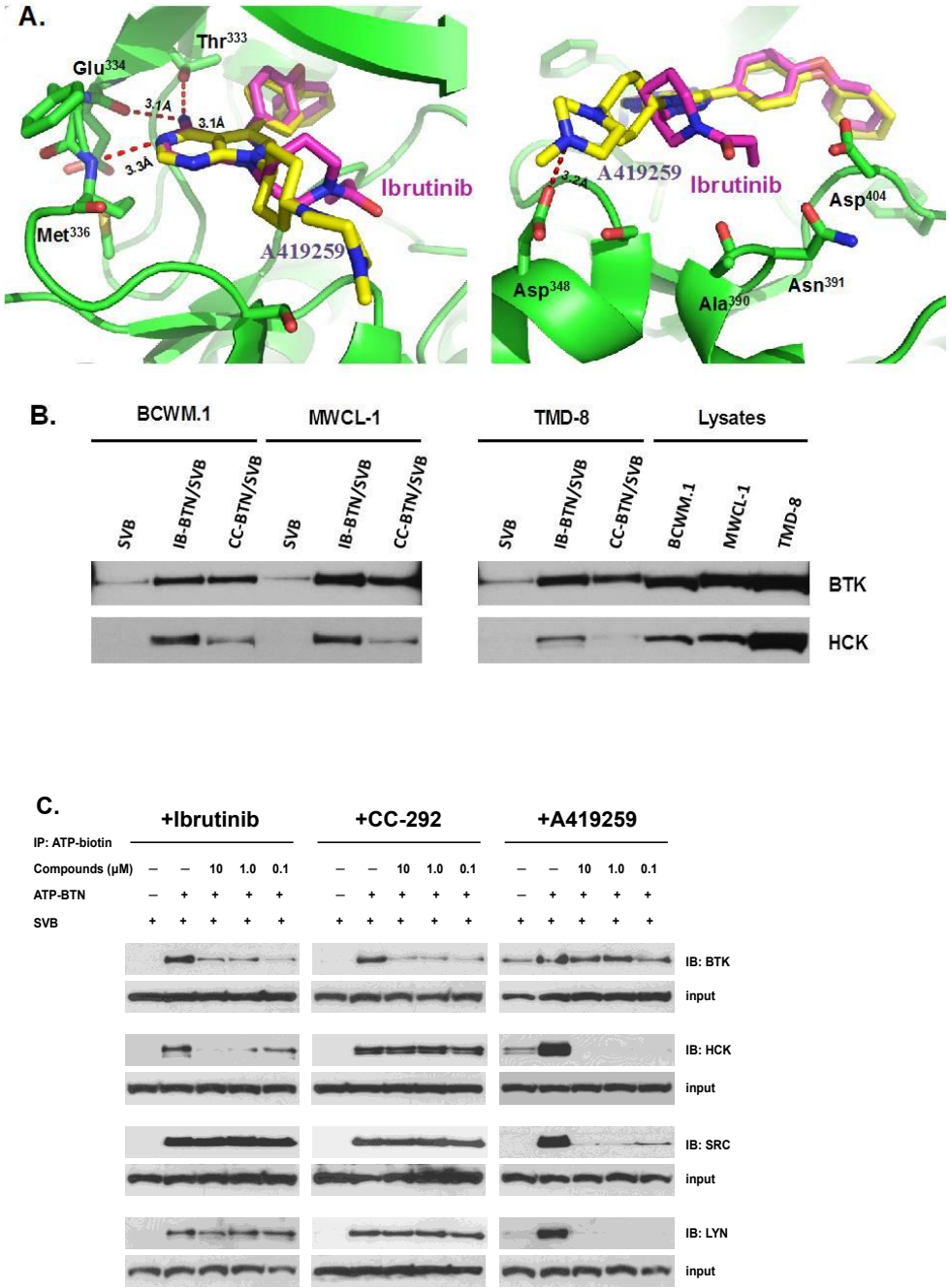
A.
Thr333
Glu334
3.1Å
3.1Å
3.3Å
Ibrutinib
A419259
Met336
A419259
Ibrutinib
Asp404
Asp348
Ala390
Asn391
B.
BCWM.1
MWCL-1
TMD-8
Lysates
SVB
IB-BTN/SVB
CC-BTN/SVB
SVB
IB-BTN/SVB
CC-BTN/SVB
SVB
IB-BTN/SVB
CC-BTN/SVB
BCWM.1
MWCL-1
TMD-8
BTK
HCK
C.
+Ibrutinib
+CC-292
+A419259
IP: ATP-biotin
Compounds (μM) – – 10 1.0 0.1 – – 10 1.0 0.1 – – 10 1.0 0.1
ATP-BTN – + + + + – + + + + – + + + +
SVB + + + + + + + + + + + + + + +
IB: BTK
input
IB: HCK
input
IB: SRC
input
IB: LYN
input

Figure 7.

A.

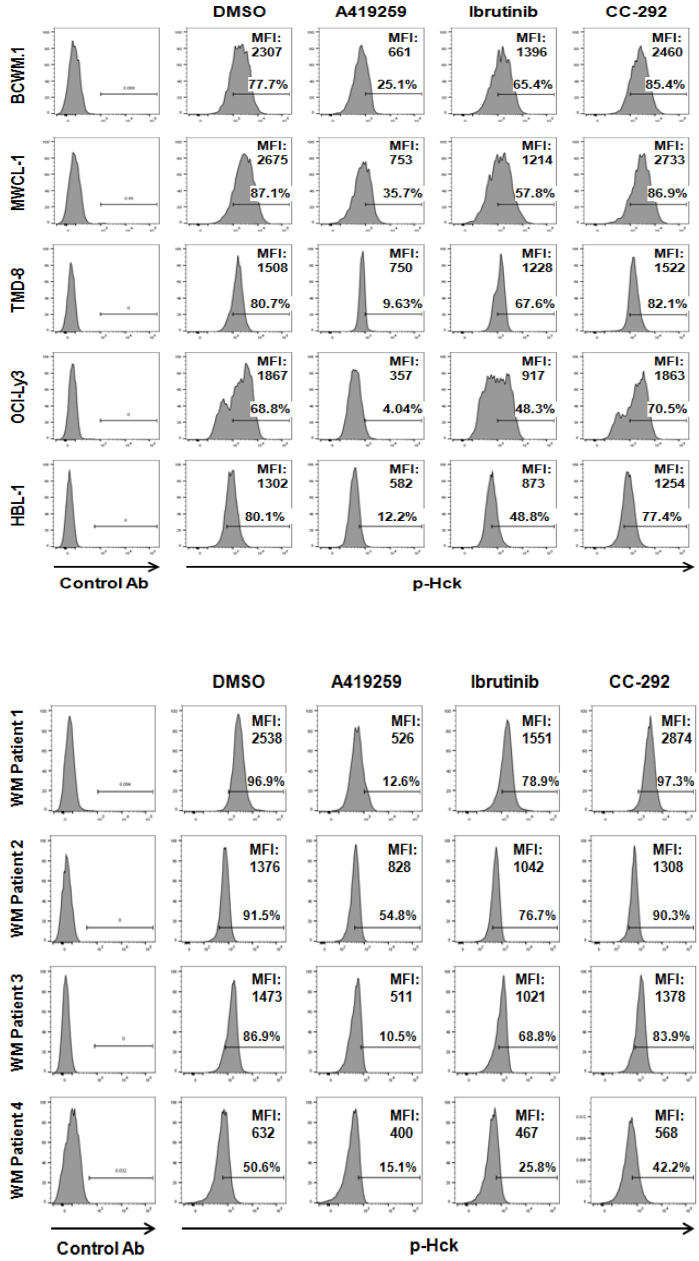
DMSO
A419259
Ibrutinib
CC-292
BCWM.1
MFI: 2307
77.7%
MFI: 661
25.1%
MFI: 1396
65.4%
MFI: 2460
85.4%
MWCL-1
MFI: 2675
87.1%
MFI: 753
35.7%
MFI: 1214
57.8%
MFI: 2733
86.9%
TMD-8
MFI: 1508
80.7%
MFI: 750
9.63%
MFI: 1228
67.6%
MFI: 1522
82.1%
OCI-Ly3
MFI: 1867
68.8%
MFI: 357
4.04%
MFI: 917
48.3%
MFI: 1863
70.5%
HBL-1
MFI: 1302
80.1%
MFI: 582
12.2%
MFI: 873
48.8%
MFI: 1254
77.4%
Control Ab
p-Hck
DMSO
A419259
Ibrutinib
CC-292
WM Patient 1
MFI: 2538
96.9%
MFI: 526
12.6%
MFI: 1551
78.9%
MFI: 2874
97.3%
WM Patient 2
MFI: 1376
91.5%
MFI: 828
54.8%
MFI: 1042
76.7%
MFI: 1308
90.3%
WM Patient 3
MFI: 1473
86.9%
MFI: 511
10.5%
MFI: 1021
68.8%
MFI: 1378
83.9%
WM Patient 4
MFI: 632
50.6%
MFI: 400
15.1%
MFI: 467
25.8%
MFI: 568
42.2%
Control Ab
p-Hck

B.

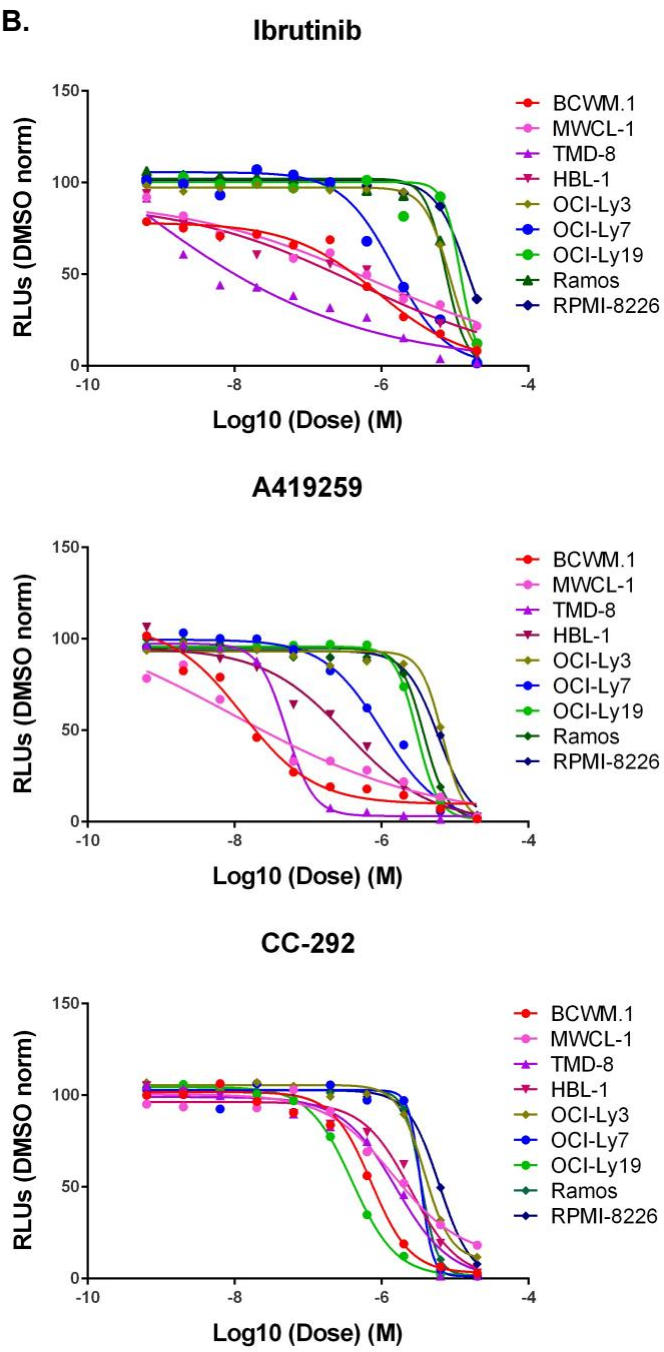
Ibrutinib
RLUs (DMSO norm)
150
100
50
0
-10
-8
-6
-4
Log10 (Dose) (M)
BCWM.1
MWCL-1
TMD-8
HBL-1
OCI-Ly3
OCI-Ly7
OCI-Ly19
Ramos
RPMI-8226
A419259
RLUs (DMSO norm)
Log10 (Dose) (M)
BCWM.1
MWCL-1
TMD-8
HBL-1
OCI-Ly3
OCI-Ly7
OCI-Ly19
Ramos
RPMI-8226
CC-292
RLUs (DMSO norm)
Log10 (Dose) (M)
BCWM.1
MWCL-1
TMD-8
HBL-1
OCI-Ly3
OCI-Ly7
OCI-Ly19
Ramos
RPMI-8226

C.

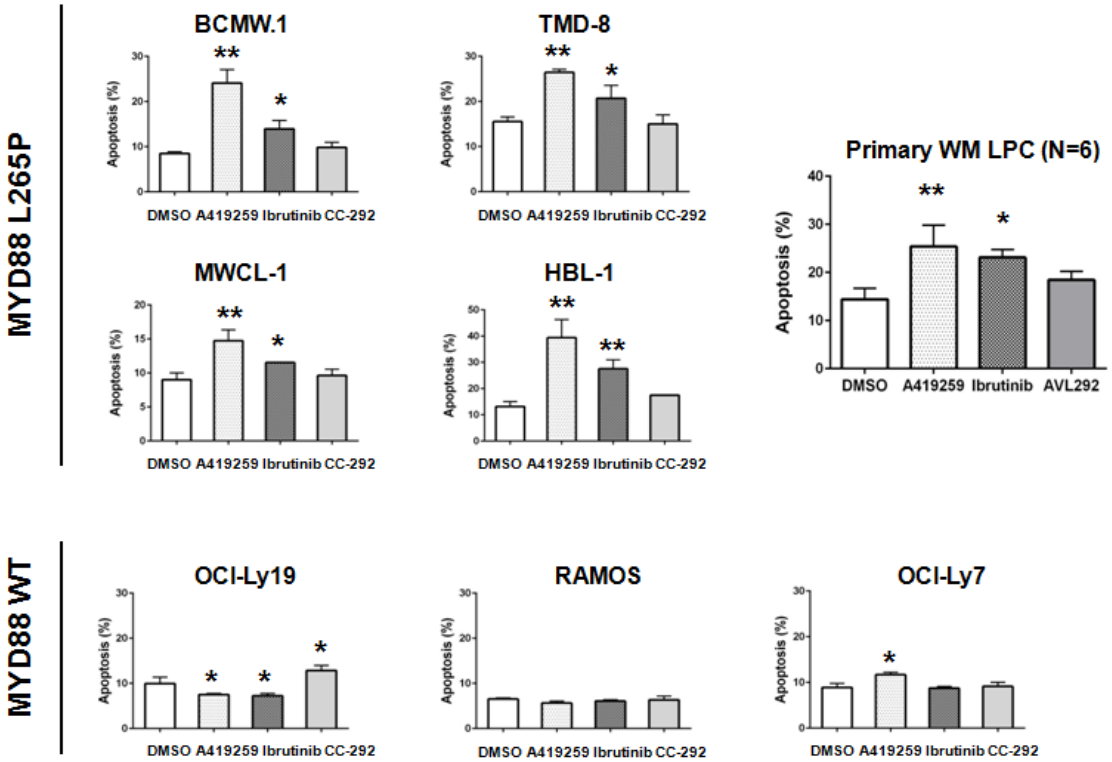
MYD88 L265P
BCMW.1
TMD-8
Primary WM LPC (N=6)
MWCL-1
HBL-1
MYD88 WT
OCI-Ly19
RAMOS
OCI-Ly7
Apoptosis (%)
DMSO A419259 Ibrutinib CC-292
DMSO A419259 Ibrutinib AVL292

D.

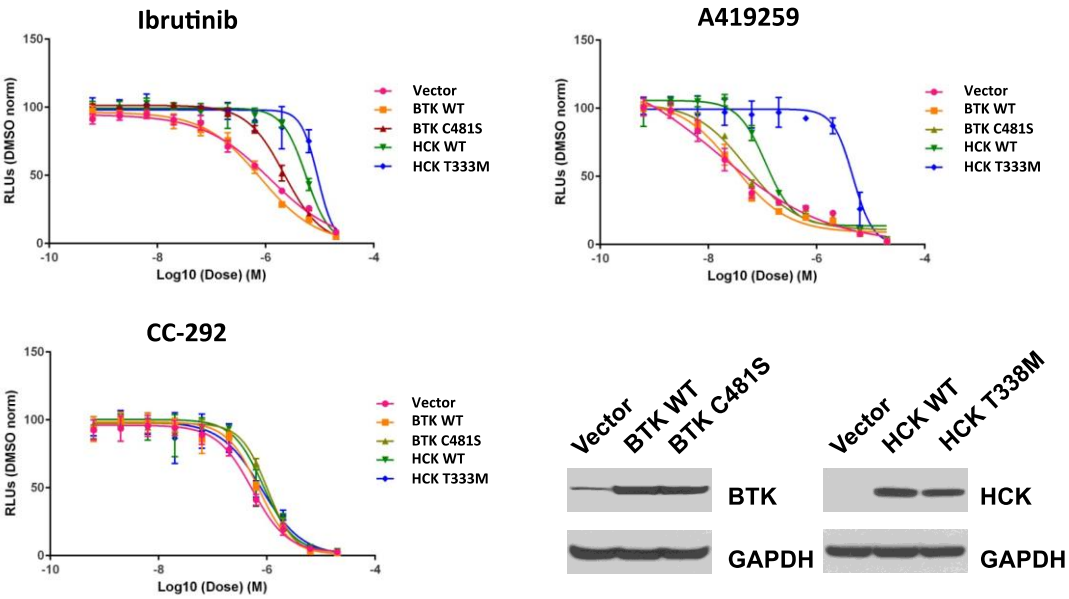
Ibrutinib
A419259
CC-292
RLUs (DMSO norm)
Log10 (Dose) (M)
Vector
BTK WT
BTK C481S
HCK WT
HCK T333M
Vector
BTK WT
BTK C481S
HCK WT
HCK T338M
BTK
HCK
GAPDH
GAPDH